15th World Congress on Computational Mechanics (WCCM-XV)
8th Asian Pacific Congress on Computational Mechanics (APCOM-VIII)
Virtual Congress: 31 July – 5 August 2022
S. Koshizuka (Ed.)

AN EFFICIENT PHASE FIELD MODEL FOR FATIGUE FRACTURE

Sikang Yan[1], **Ralf Müller**[2]

[1] University of Kaiserslautern, Gottlieb-Daimler-Straße, 67655 Kaiserslautern, Germany,
yan@rhrk.uni-kl.de

[2] Technical University of Darmstadt, Franziska-Braun-Straße 7, 64287 Darmstadt,
ralf.mueller@mechanik.tu-darmstadt.de

Key words: phase field, fatigue fracture, effcient

Abstract. The fatigue phenomenon is difficult to be modeled and simulated because of its natural property, which does not happen imminently but rather after a larger number of cycles. Usually, the simulation of fatigue fracture behavior also requires a lot of computation effort which can be seen as very time-consuming. In this work, we represent an efficient phase field model aiming to handle the cyclic fatigue fracture.

1 INTRODUCTION

The core idea of the phase field model is to represent a discrete, discontinuous phenomenon with a smooth function. For fracture mechanics an additional field variable is introduced to describe the crack. The biggest advantage of the phase field fracture model is its unified framework of the entire crack evolution behavior, including nucleation, propagation, branching, kinking. These phenomena can be covered by one single model. The phase field fracture has been successfully applied to a quasi-statics case. However, there is still a lack of studies on how to efficiently simulate the fatigue fracture phenomenon. In this work, we propose an efficient phase field schemata for cyclic fatigue simulation.

We extend the model from Kuhn and Müller [1] with an additional potential energy term, which provides the necessary driving force for the fatigue fracture evolution. This additional potential is related to the newly introduced damage parameter, representing the damage caused by cyclic fatigue. The additional potential energy is coupled with fatigue parameters from the S-N diagram, which allows the model to generally and elegantly integrate all the influence from the environment to the fatigue propagation behavior. The evolution of the crack field is derived from the total energy with the help of variational principle. The model is consistent with the empirical fatigue propagation property and also robust under complex load simulations.

Traditionally, the fatigue simulation suffers from its huge computational effort since the fatigue crack will only occur after a large number of loading cycles. The cycle number increment influences the computing time of the fatigue simulation and impacts the crack patterns. Thus, the cycle number increment choice is a critical point in the phase field fatigue simulation. We introduce an adaptive cycle increment algorithm, where the cycle number increment is associated with the fatigue damage increment. Our algorithm provides a moderate computing time without losing accuracy compared to the classical computing strategies. Our method is also suitable for parallel computing.

The model has been applied to three-dimensional problems with the real material property. The fatigue life obtained from the phase field model can be verified by experimental and analytical findings.

2 A PHASE FIELD MODEL FOR FATIGUE

A phase field fracture model introduces an additional field variable to represent cracks. In the phase field model from [1] for a quasi-static case, the crack field s is 1 if the material remains undamaged and is 0 where cracks occur. Furthermore, it is to postulate that the displacement field $\mathbf{u}$ and crack field s locally minimize the total energy of a loaded body Ω. The total energy $\mathcal{E}$ is given as

$$\mathcal{E} = \mathcal{E}^e + \Gamma, \tag{1}$$

where $\mathcal{E}^e$ is the elastic strain energy, which is the energy stored inside of an elastic body. With ψ^e denoting the elastic strain energy density, the elastic strain energy is given as

$$\mathcal{E}^e = \int_\Omega (g(s)+\eta)\psi^e \mathrm{d}V = \int_\Omega \frac{1}{2}\Big((g(s)+\eta)\boldsymbol{\varepsilon} : [\mathbb{C}\boldsymbol{\varepsilon}]\Big)\mathrm{d}V. \tag{2}$$

The degradation function $g(s)$ models the loss of the stiffness of the broken material. η is a dimensionless parameter used to avoid numerical difficulties, $\boldsymbol{\varepsilon}$ is the infinitesimal strain tensor and $\mathbb{C}$ is the stiffness tensor. The fracture surface energy representing the energy to separate the material to generate cracks, is assumed to be proportional to the broken surface area A_s

$$\Gamma = \int_\Omega \psi^s \mathrm{d}V = \mathcal{G}_c A_s, \tag{3}$$

where $\mathcal{G}_c$ is the cracking resistance, which models the ability of a material to resist fracturing; and ψ^s is the fracture surface energy density. With the surface density functional, which is related to the gradient of the crack ∇s and the crack s itself, the fracture surface energy is given as

$$\Gamma = \int_\Omega \mathcal{G}_c\left(\frac{(1-s)^2}{4\varepsilon} + \varepsilon|\nabla s|^2\right)\mathrm{d}V. \tag{4}$$

When ε comes close to zero, the surface density functional approximates the fracture surface. The length parameter ε controls the width of the transition zone between the broken and undamaged material.

In order to include the fatigue fracture feature in the phase field model, we extend the phase field model from [1] by an additional term for cyclic fatigue. The phase field model for fatigue fracture now reads

$$\mathcal{E} = \mathcal{E}^e + \Gamma + \mathcal{P}, \tag{5}$$

where $\mathcal{P}$ stands for an additional free energy term for the sum of additional driving forces caused by fatigue damage. This additional fatigue energy consists of two parts

$$\mathcal{P} = \int_\Omega h(s)\psi^{\mathrm{ad}}(D) = \int_\Omega h(s) q <D - D_c>^b, \tag{6}$$

where $h(s)$ is a degradation function, which models the loss of stiffness of broken material caused by cyclic fatigue. ψ^{ad} is the fatigue energy density, which provides additional driving forces for cyclic fatigue. The fatigue energy density is related to a fatigue damage parameter D. This concecpt of cumulative damage model inspired by Miner's rule [2], in which the damage parameter will be continuously accumulated during the simulation

$$D_{\mathrm{n}+1} = D_0 + \mathrm{d}D_{\mathrm{n}}, \tag{7}$$

where D_0 is the previous fatigue damage of the last simulation iteration. The quantity dD is the damage increment, which is associated with the cycle increment in the fatigue simulation

$$\mathrm{d}D = \mathrm{d}N \frac{1}{n_D} \left(\frac{\hat{\sigma}}{A_D} \right)^k . \tag{8}$$

D_c is a damage threshold. The parameters A_D, k and n_D can be obtained from the S-N curve. The term $\hat{\sigma}$ is the driving force for the fatigue crack propagation, corresponding to the first principal stress of the stress tensor $\boldsymbol{\sigma} = \mathbb{C}\boldsymbol{\varepsilon}$ in this case. The Macauley brackets

$$\langle x \rangle^n = \begin{cases} 0 & \text{if} \quad x \leq 0 \\ x^n & \text{if} \quad x > 0, \end{cases} \tag{9}$$

allows the fatigue energy term takes contribution into total energy density only when the damage parameter D reaches the damage threshold D_c. After that, the regularization parameters q and b determine the speed of fatigue damage energy growth. Allocating all above definitions, the additional fatigue energy density reads

$$\psi^{\mathrm{ad}} = h(s) q < D_0 + \frac{\mathrm{d}N}{n_D} \left(\frac{\hat{\sigma}}{A_D} \right)^k - D_c >^b . \tag{10}$$

It is to postulate that the displacement field and crack field minimize the total energy $\mathcal{E}$ (Eq. (5)), which yields the entire crack propagation behavior. In recent work, the phase field model can be adapted to a more general form with a mean stress correction term, which allows the mean effect of materials to be included [3] [4].

The phase field model is capable to recapture different important fatigue features. The growth behavior of a macro crack can be described by Paris' law [5], which describes the fatigue crack growth rate in relation to the stress intensity factor range. It is to notice that according Paris' law the relation between crack growth rate and crack intensity factor range will be displayed as a straight line on a logarithmic scale. Figure 1 shows the crack growth rate for different levels of maximum stress amplitude. Even if different stress amplitudes for the simulation are applied, the rate of crack growth can be described with the same Paris' law. Radhakrishnan [6] shows that the constant C and the slope m depend on the mean stress of the load in some materials. Figure 2 displays the effect of mean stress on the crack growth rate, where the stress ratio R is defined as the ratio between the minimum stress and the maximum stress. The depicted diagram reflects that higher mean stress increases the rate of crack growth. Figure 3 reports the effect of the loading sequence on the crack growth rate. Results show that a high-low loading sequence results in short fatigue life. This phenomenon is called the loading sequence effect. It has been shown that the material with a low-high load sequence results in a longer fatigue life. It is because the low load level is mostly involved in the crack nucleation and the high load level is contributed to the crack propagation [7]. Although Miner's rule does not include the loading sequence effect, the damage quantity D with a low load level reaches later the critical damage state D_c in the phase field model.

3 ACCELERATION METHOD IN PHASE FIELD SIMULATION

Traditionally, the fatigue simulation suffers from its huge computational effort. In order to reduce the computing time and without losing accuracy, two acceleration approaches are applied in the phase

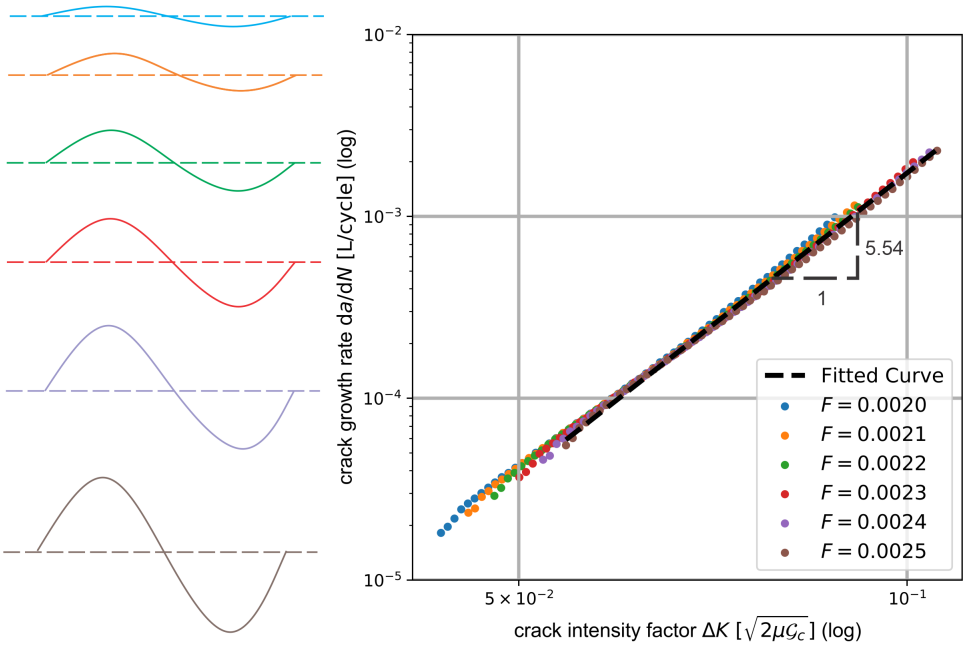

Figure 1: crack growth rate for different levels of maximum stress amplitude.

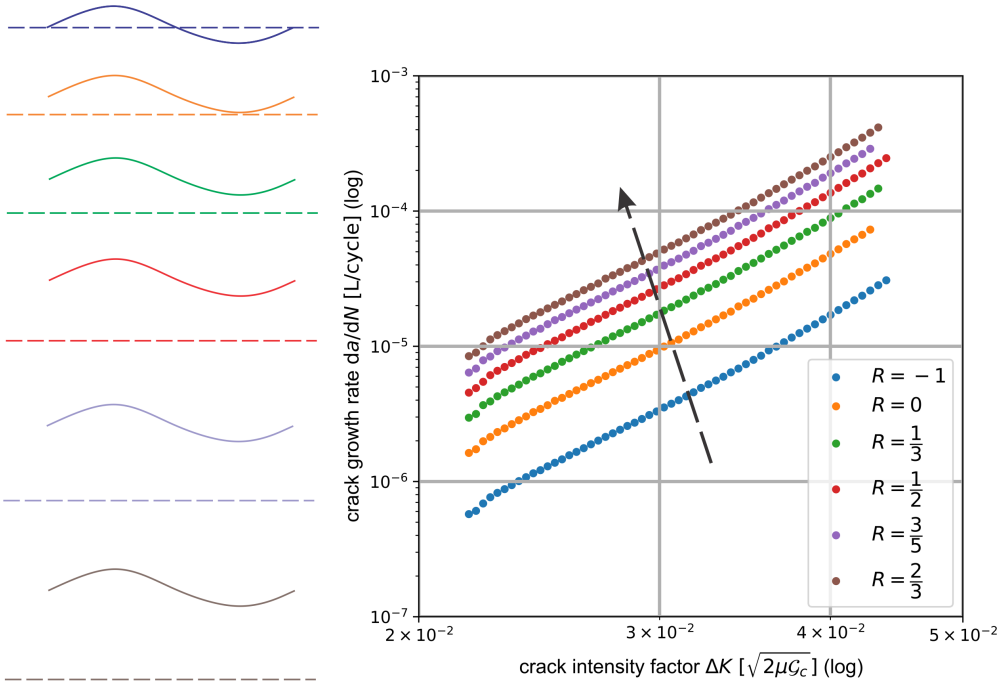

Figure 2: load sequence effect on the fatigue life.

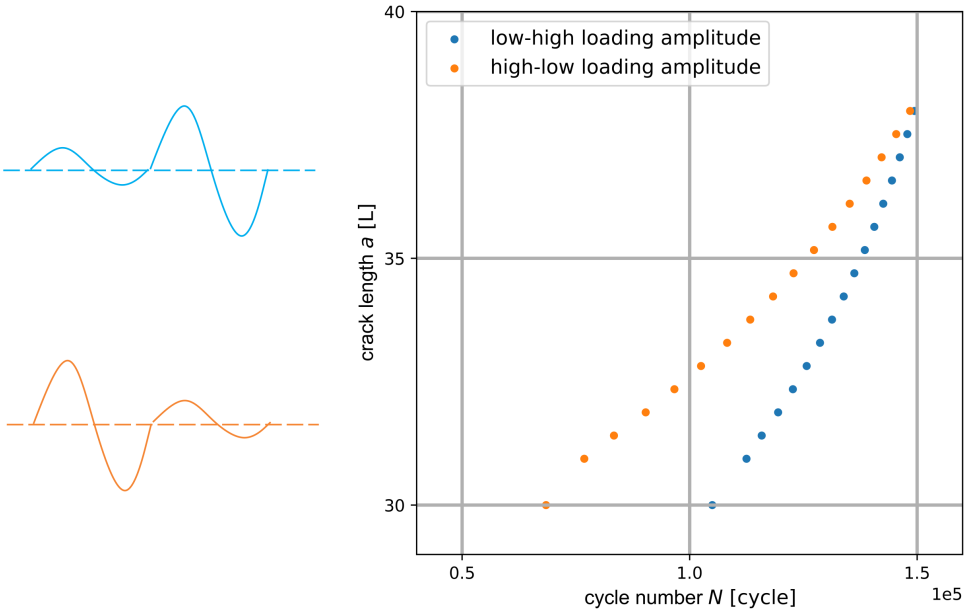

Figure 3: crack growth rate for different mean stress ratios.

field simulation: **a**daptive **c**ycle **n**umber **a**djustment **a**lgorithm (*ACNAA*) and parallel computing(message passing interface *MPI*). One is based on the algorithmic perspective and the other is on the programming perspective.

3.1 Adaptive cycle number adjustment algorithm (*ACNAA*)

In contrast to other fracture phenomena, fatigue damage occurs only after a large number of load cycles. This requires a large amount of computational effect in the simulations. In addition, the choice of the number of cycles is usually determined by a compromise between simulation time and its accuracy. The choice of the increment of the number of cycles is a key point of the phase field fatigue model: not only because it determines the simulation time, but also strongly influences the shape of the crack. If the cycle number increment is too large, the crack trace is very wide and irregular. Moreover, too large cycle increments cause a sharp increase in fatigue energy, which can lead to an unstable energy state in the simulation [4].

In the phase field model, the damage parameter D is introduced to model the damage of the material related to fatigue. The idea of the adaptive cycle number adjustment algorithm is to associate the cycle number increment with the damage increment of each simulation iteration. According to the damage state, the simulation of fatigue fracture is divided into three stages:

① the fatigue damage is below the fatigue damage threshold $D < D_c$: The fatigue energy term vanishes at this stage, thus it can be seen as a pure static mechanical state. The cycle increment should be chosen as large as possible in order to quickly reach the critical fatigue state.

② the fatigue damage is near the fatigue damage threshold $D \approx D_c$: At this moment, the material is

about to break and the cycle number increment dN should be chosen in such a way that the damage increment dD small enough to simulate the transient process.

③ the fatigue damage is above the fatigue damage threshold $D > D_c$: After the fatigue damage is over the fatigue damage threshold, the fatigue damage begins. At this stage, the maximum damage increment max[dD] of the entire computation domain is regulated in order to obtain a moderate growth rate of the fatigue energy.

Fig. 4 illustrates how the ACNAA works. It has been shown that the computing time can drop to nearly 3% using our method, compared to constant cycle number increment with d$N = 5$ [4].

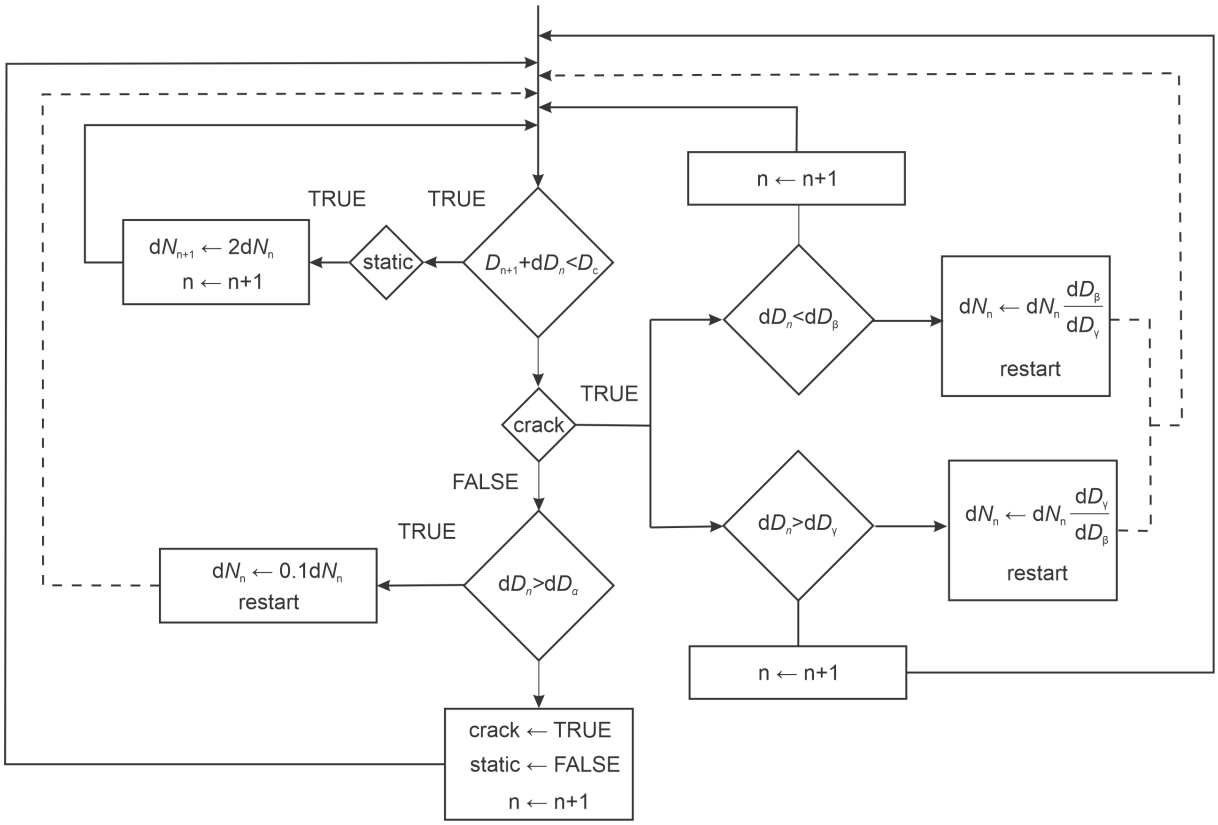

Figure 4: The idea of ACNAA is to divide the entire fatigue simulation into three stages and associate the cycle increment with damage increment. D_α, D_β and D_γ are the numerical parameters for the algorithm.

3.2 Parallel computing (MPI)

For a large and complicated problem raised in the computational science domain, using a single processor to sequentially complete the task is usually not suited. Parallel computing breaks down the large problem into smaller, independent parts and executes them simultaneously by communicating with multiple processors. One of the parallelization concepts is via the message passing interface.

The message-passing model uses a set of processors, which only have local memory; however, these processors are capable to communicate with each other by sending and receiving messages. In infinite

element computing, the huge number of finite elements is processed by multiple processors simultaneously, where the information and memory during the parallel computing can be shared via message passing among all the processors. The entire mesh is after a sequential computing **forked** into different pieces of small meshes, which will be computed individually by every processor; and after this parallel computing phase, the information, the result as well as the mesh will be **joined** again as a single task. This is the so-called "fork-and-join" strategy in parallel computing (see Fig. 5).

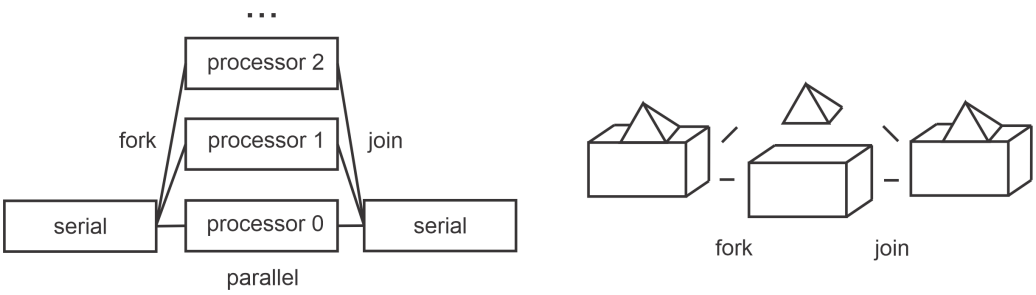

Figure 5: The "fork-and-join" concept.

Figure 6 reports the computing time to the number of processors in 2D problems (Fig. 6**a**) as well as 3D problems (Fig. 6**b**), where the Newton's method is separately solved with the direct solver (MUMPS) and the iterative solver (CG with preconditioner hyper_amg) in each case. It is clear to observe that increasing the number of processors reduces the computing time in most cases. Parallel computing with 8 processes only requires around 8 hours to complete the task for a 3D problem, which is only 2% of the time compared to sequential computing. The speed-up performance reveals differently, depending on the type of Newton's method as well as the dimension of the problem: for a 2D problem, the MUMPS solver can dramatically accelerate the simulation when the number of processors from 1 raising to 4; however, it requires even more time when using 8 processors. On the other side, parallel computing works effectively by using 2 processors with the CG solver. In contrast to the two-dimensional cases, the speed-up is obvious for 3D simulation when the number of processors rises no matter which solver is used.

This contrastive performance might be explained by Amdahl's law [8]. The productivity of the phase field simulation program can not be improved further due to the overhead of parallelism, like the synchronizations, the data communications, etc.. Weighing the gains and losses, the best paralleling strategy is to use a MUMPS solver with 4 processors for a small task (e.g. 2D problems) or 8 processors for a complex task.

It is to be noticed that the adaptive cycle number adjustment algorithm needs to be modified in order to be suited to a parallel algorithm. Only the main processor has access to adjust the damage increment dD and the cycle increment dN in each simulation iteration to avoid synchronization issues. The cycle numbers N will be synchronized and broadcast to the other processors after the cycle increment is adjusted by the main processor.

4 NUMERICAL EXAMPLES

The phase field fatigue model is tested with different loading scenarios and the results are demonstrated in this section. The first example is the block geometry adapted from SPP-1748 Benchmark [9]. This

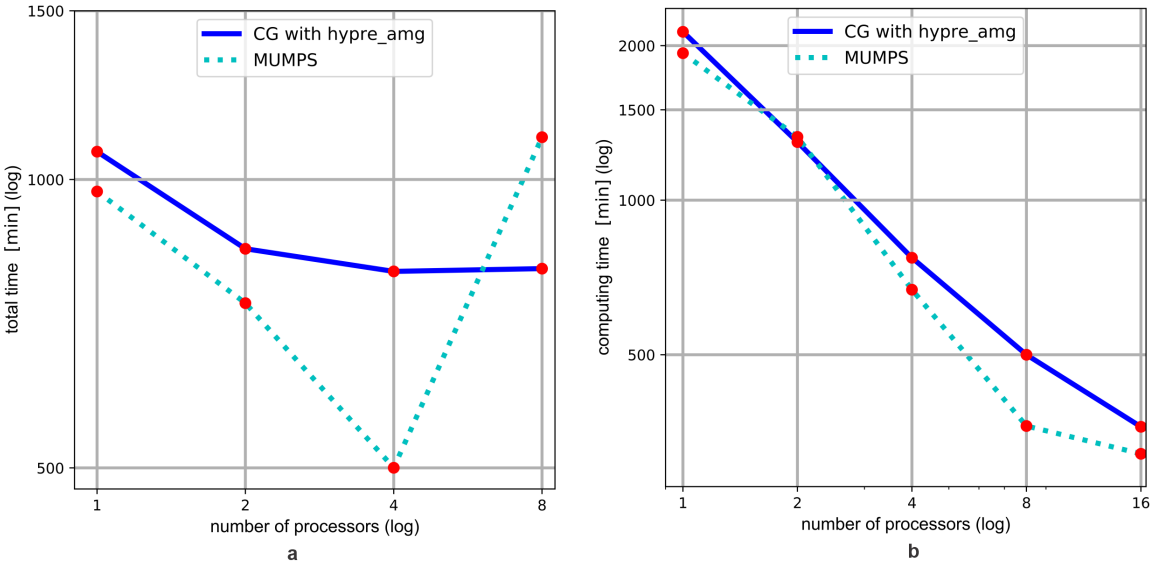

Figure 6: The computing time with help of parallel computing in 2D (**a**) and 3D (**b**).

example is straightforward and disregards particular distinction problems between tension and compression since the cracks should only occur in the tension region. A specific area of its top surface (marked in red) is loaded with a prescribed displacement, and the bottom of the box is fixed. Furthermore, to distinguish this loading situation from a simple monotonous pure tension loading, we assume this loaded area of top surface will never be broken. It is to notice the crack begins at the top surface of the box as shown in Fig. 7, which is different from the pure elastic shown in [9]. The reason for these differences is that the first principal stress is the driving force in phase field fatigue model, the crack extends as the maximum first principal stress is found.

Our model has also been tested with CT specimen in different fracture modes (see Fig. 8). The material of the CT specimen is assumed to be AISI316L stainless steel, where the material parameters are taken from [10] [11] [12]. The crack patterns are varied as long as the loading is in different fracture modes: the direction of the crack propagation from mode I is horizontal (0°); from mode II is around 55° and mode III is around 70°. These different propagation behaviors are predicted by the principal stress and the strain energy density criteria and can be verified by the experiment findings [13] [11] as well as the analytical calculation [14]. Based on the maximum tangential stress (*MTS*) criterion from Erdogan et al. [14], the crack grows in a direction where it has the maximum tangential stress σ_θ and the shear stress $\tau_{r\theta}$ vanishes. The stress components of a straight extending crack tip in a 2 dimensional cylindrical

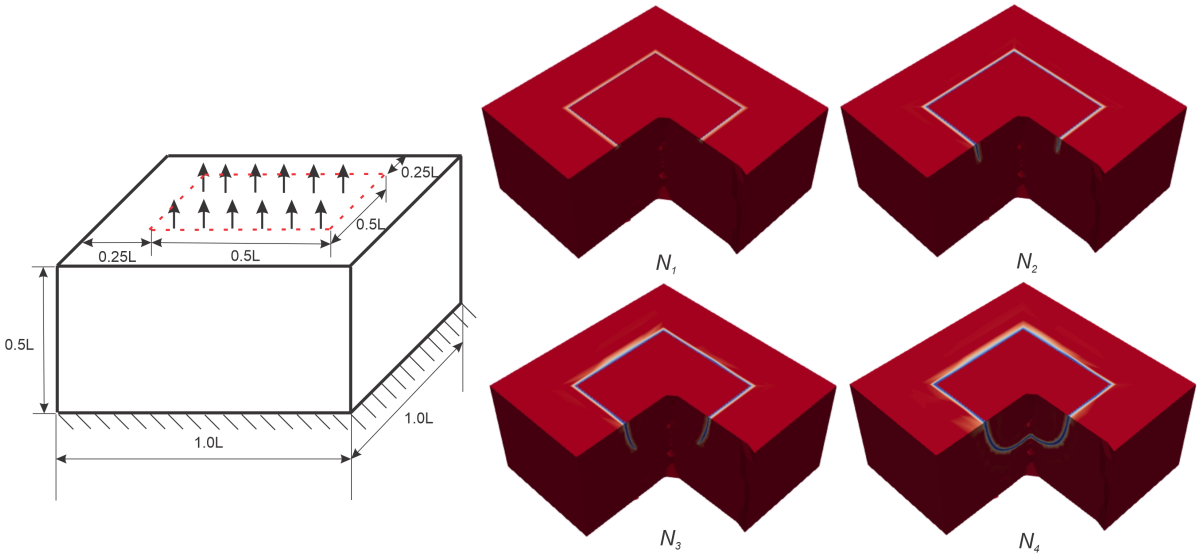

Figure 7: The crack evolution of a 3d block geometry.

coordinate setting is given in [14]

$$\sigma_r = \frac{1}{\sqrt{2r}}\cos\frac{\theta}{2}\left[k_1\left(1+\sin^2\frac{\theta}{2}\right)+\frac{3}{2}k_2\sin\theta-2k_2\tan\frac{\theta}{2}\right] \tag{11}$$

$$\sigma_\theta = \frac{1}{\sqrt{2r}}\cos\frac{\theta}{2}\left[k_1\cos^2\frac{\theta}{2}-\frac{3}{2}k_2\sin\theta\right] \tag{12}$$

$$\tau_{r\theta} = \frac{1}{2\sqrt{2r}}\cos\frac{\theta}{2}[k_1\sin\theta+k_2(3\cos\theta-1)], \tag{13}$$

where k_1 and k_2 are the symmetric and skew-symmetric components of the stress intensity factors and r and θ are the radial and angular coordinates of the crack tip. For the mode I loading situation, only the symmetric-part of stress intensity factor remains $k_2 = 0$, which leads to the horizontal crack propagation behavior

$$\theta = 0^\circ. \tag{14}$$

As in the theoretical analysis of the mode II and mode III loading situation, the stress state is skew-symmetric with $k_1 = 0$. The angle of crack extension θ can be obtained from Eq. (11)

$$\theta = -\arccos\frac{1}{3} = -70.5^\circ. \tag{15}$$

The derivation of fracture mode II from the phase field simulation and theoretical calculation can be explained by the mixed stress situation due to the complex geometry of CT specimen. The crack angle in those situations can be determined from the maximum tangential stress with the relation

$$k_1\sin\theta+k_2(3\cos\theta-1) = 0. \tag{16}$$

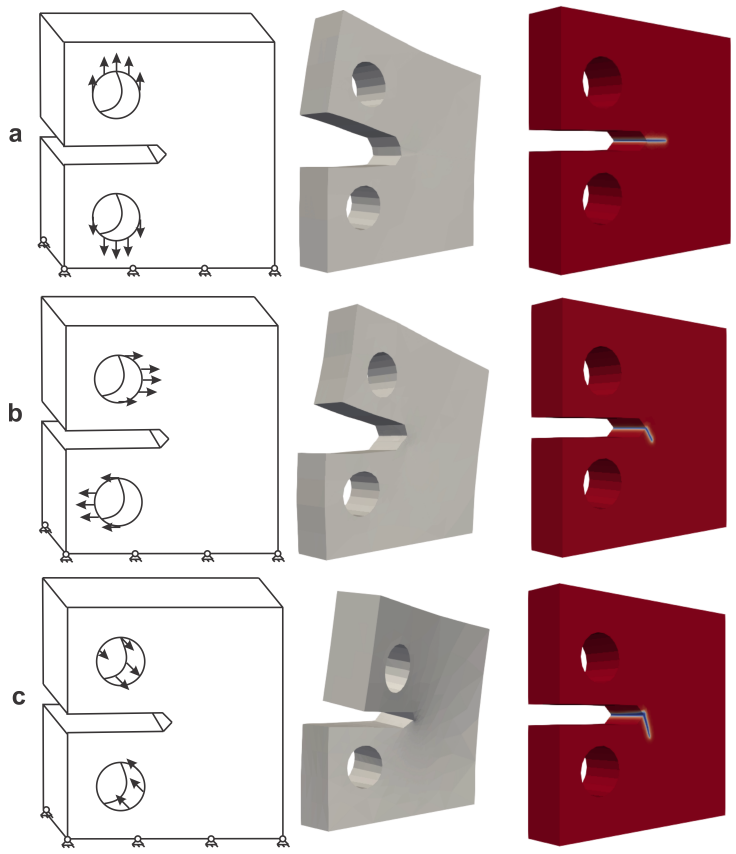

Figure 8: CT specimen under different fracture modes: **a**: mode I; **b**: mode II; **c**: mode III.

5 CONCLUSION

In this work, a phase field model for cyclic fatigue is presented. Originally, only the elastic energy and fracture surface energy are considered in the phase field fracture model. To incorporate the fatigue situations, we introduce an additional fatigue energy term accounting for the fatigue driving force into the total energy density. The entire crack propagation behavior can be derived by minimizing the extended total energy equation. Due to the natural property of fatigue fracture, which happens not immediately, the phase field simulation always requires a huge number of computational effects. In this work, we provide two computation accelerations methods, which lie in the algorithm and programming points of view. Results show that the phase field model is capable to handle complex fatigue fracture scenarios. In future work, the internal friction and thermal fatigue are going to be built into the phase field model.

6 ACKNOWLEDGEMENTS

Funded by the Deutsche Forschungsgemeinschaft (DFG, German Research Foundation) – 252408385 –IRTG 2057

REFERENCES

[1] *Kuhn, C. and Müller, R., "A continuum phase field model for fracture", Eng. Frac. Mech., 48(4):797-826, (2000).*

[2] *Miner, M. A.,"Cumulative damage in fatigue", (1945).*

[3] *Schreiber, C., Müllerr R. and Kuhn C., "Phase field simulation of fatigue crack propagation under complex load situations", Arch. of Appl. Mech., pp. 1–15, (2020).*

[4] *Yan, S., Schreiber, C. and Müllerr R., "An efficient implementation of a phase field model for fatigue crack growth", Int. Jour. of Frac, pp. 1–14, (2022).*

[5] *Paris, P. and Erdogan, F.,"A critical analysis of crack propagation laws", (1963)*

[6] *Radhakrishnan, V.,"arameter representation of fatigue crack growth", Eng. Frac. Mech. vol. 11, no. 2, pp. 359–372, (1979).*

[7] *Ralph, I. S., Ali, F., Robert, R. S. and Henry, O. F., "Metal fatigue in engineering", (2000).*

[8] *Amdahl, G. M., "Validity of the single processor approach to achieving large scale computing capabilities", IEEE Soli.-St. Circ. Soci. News. 12.3: 19-20, (2007).*

[9] *Müllerr, R. and Kuhn C., "Spp-1748 benchmark collection phase field", (2020).*

[10] *Boyer, H. E. and Gall, T. L., "Metals handbook; desk edition", (1985).*

[11] *Mohammad, K. A., Zainudin, E. S., Sapuan, S., Zahari, N. I. and Aidy, A., "Fatigue life for type 316l stainless steel under cyclic loading", vol. 701, pp. 77–81, (2013).*

[12] *Roylance D., "Introduction to fracture mechanics" (2001).*

[13] *Song, S. H. and Lee, J. M., "Mode ii fatigue crack behavior in compact tension shear specimen," in Key Eng. Mat., vol. 297, pp. 1592–1597, Trans. Tech. Publ., (2005).*

[14] *Erdogan, F. and Sih, G., "On the crack extension in plates under plane loading and transverse shear," (1963).*